Special Report

Chinese expert consensus on imaging diagnosis of drug-resistant pulmonary tuberculosis

Chuan-Jun Xu[1#], Pu-Xuan Lu[2#], Chun-Hua Li[3#], Yu-Lin He[4#], Wei-Jun Fang[5#], Ru-Ming Xie[6], Guan-Qiao Jin[7], Yi-Bo Lu[8], Qiu-Ting Zheng[2], Guang-Ping Zheng[9], Sheng-Xiu Lv[3], Hua Huang[9], Li Li[10], Meiji Ren[10], Yu-Xin Shi[11], Xin-Nian Wen[12], Lin Li[13], Fang-Jun Wei[9], Dai-Lun Hou[14], Yan Lv[14], Fei Shan[11], Zheng-Can Wu[15], Zhi-Liang Hu[16], Xiang-Rong Zhang[17], Du-Xian Liu[18], Wei-Ya Shi[11], Hui-Ru Li[5], Na Zhang[19], Min Song[5], Xin Zhang[20], Ying-Ying Deng[21], Jinlong Li[22], Qiang Liu[23], Dechun Li[24], Lingling Zhao[25], Bu-Dong Chen[26], Yan-Bin Shi[27], Feng-Li Jiang[28], Xin Tang[29], Li-Ji Wu[30], Wei Ma[31], Xin-Yue Xu[32], Hong-Jun Li[10]

[1]Department of Radiology, The Second Hospital of Nanjing, Nanjing University of Chinese Medicine, Nanjing, China; [2]Department of Medical Imaging, Shenzhen Center for Chronic Disease Control, Shenzhen, China; [3]Department of Radiology, Chongqing Public Health Medical Center, Chongqing, China; [4]Department of Radiology, The First Affiliated Hospital of Nanchang University, Nanchang, China; [5]Department of Radiology, Guangzhou Chest Hospital, Guangzhou, China; [6]Department of Radiology, Beijing Ditan Hospital, Capital Medical University, Beijing, China; [7]Department of Radiology, The Affiliated Cancer Hospital of Guangxi Medical University, Nanning, China; [8]Department of Radiology, The Fourth People's Hospital of Nanning, Nanning, China; [9]Department of Radiology, The Third People's Hospital of Shenzhen, Shenzhen, China; [10]Department of Radiology, Beijing You'an Hospital, Capital Medical University, Beijing, China; [11]Department of Radiology, Shanghai Public Health Clinical Center, Shanghai, China; [12]Department of Medical Imaging, Chest Hospital of Guangxi Zhuang Autonomous Region, Liuzhou, China; [13]Department of Radiology, Linyi People's Hospital, Linyi, China; [14]Department of Medical Imaging, Beijing Chest Hospital, Capital Medical University, Beijing, China; [15]Department of Radiology, Nanjing First Hospital, Nanjing Medical University, Nanjing, China; [16]Department of Infectious Disease, The Second Hospital of Nanjing, Nanjing University of Chinese Medicine, Nanjing, China; [17]Department of Pulmonary Tuberculosis, The Second Hospital of Nanjing, Nanjing University of Chinese Medicine, Nanjing, China; [18]Department of Pathology, The Second Hospital of Nanjing, Nanjing, China; [19]Department of Radiology, Public Health and Clinical Center of Chengdu, Chengdu, China; [20]Department of Medical Imaging, The Fourth People's Hospital of Huai'an, Huai'an, China; [21]Department of Radiology, Shenzhen Yantian District People's Hospital, Shenzhen, China; [22]Department of Laboratory Medicine, The Second Hospital of Nanjing, Nanjing University of Chinese Medicine, Nanjing, China; [23]Department of Radiology, Shandong Provincial Hospital, Shandong First Medical University, Jinan, China; [24]Department of Radiology, Xuzhou Central Hospital, Xuzhou, China; [25]Department of Radiology, The Sixth Peoples Hospital of Zhengzhou, Zhengzhou, China; [26]Medical Imaging Quality Research Committee, China Quality Association for Pharmaceuticals, Beijing, China; [27]Department of Radiology, The Sixth Peoples Hospital of Zhengzhou, Zhengzhou, China; [28]Department of Radiology, Zhejiang Cancer Hospital, Hangzhou, China; [29]Department of Radiology, The First Affiliated Hospital of Nanchang University, Nanchang, China; [30]Department of Imaging, Fourth Hospital of Inner Mongolia Autonomous, Hohhot, China; [31]Department of Radiology, The Third People's Hospital of Longgang, Shenzhen, China; [32]The School of Radiation Medicine and Protection (SRMP) of Soochow University, Suzhou, China

Contributions: (I) Conception and design: All authors; (II) Administrative support: All authors; (III) Provision of study materials or patients: All authors; (IV) Collection and assembly of data: All authors; (V) Data analysis and interpretation: All authors; (VI) Manuscript writing: All authors; (VII) Final approval of manuscript: All authors.

[#]These authors contributed equally to this work as co-first authors.

Correspondence to: Hong-Jun Li, MD. Department of Radiology, Beijing You'an Hospital, Capital Medical University, No. 8, Xitoutiao, You'an Gate, Fengtai District, Beijing 100000, China. Email: lihongjun00113@ccmu.edu.cn; Pu-Xuan Lu, MD. Department of Medical Imaging, Shenzhen Center for Chronic Disease Control, No. 2021, Buxin Road, Luohu District, Shenzhen 518020, China. Email: lupuxuan@126.com.

Abstract: Tuberculosis (TB) remains one of the major infectious diseases in the world with a high incidence rate. Drug-resistant tuberculosis (DR-TB) is a key and difficult challenge in the prevention and treatment of TB. Early, rapid, and accurate diagnosis of DR-TB is essential for selecting appropriate and personalized

treatment and is an important means of reducing disease transmission and mortality. In recent years, imaging diagnosis of DR-TB has developed rapidly, but there is a lack of consistent understanding. To this end, the Infectious Disease Imaging Group, Infectious Disease Branch, Chinese Research Hospital Association; Infectious Diseases Group of Chinese Medical Association of Radiology; Digital Health Committee of China Association for the Promotion of Science and Technology Industrialization, and other organizations, formed a group of TB experts across China. The conglomerate then considered the Chinese and international diagnosis and treatment status of DR-TB, China's clinical practice, and evidence-based medicine on the methodological requirements of guidelines and standards. After repeated discussion, the expert consensus of imaging diagnosis of DR-PB was proposed. This consensus includes clinical diagnosis and classification of DR-TB, selection of etiology and imaging examination [mainly X-ray and computed tomography (CT)], imaging manifestations, diagnosis, and differential diagnosis. This expert consensus is expected to improve the understanding of the imaging changes of DR-TB, as a starting point for timely detection of suspected DR-TB patients, and can effectively improve the efficiency of clinical diagnosis and achieve the purpose of early diagnosis and treatment of DR-TB.

Keywords: Pulmonary tuberculosis (PTB); drug resistance; tomography; X-ray computer; imaging diagnosis; expert consensus

Submitted Aug 27, 2023. Accepted for publication Sep 23, 2023. Published online Oct 25, 2023.
doi: 10.21037/qims-23-1223
View this article at: https://dx.doi.org/10.21037/qims-23-1223

Introduction

Tuberculosis (TB) ranks 13th in the world as a cause of death (1). In 2021, there were 10.6 million new cases of TB worldwide. The burden of drug-resistant tuberculosis (DR-TB) also increased in 2020–2021. Among the new TB patients in 2021, there were 450,000 cases of rifampicin-resistant tuberculosis (RR-TB). The number of RR-TB and multidrug-resistant tuberculosis (MDR-TB) patients reported to have received appropriate treatment in 2021 is 161,746, covering only 1/3 of all patients requiring treatment. The current global treatment success rate for DR-TB is 60%, which is still very low. DR-TB remains a major public health problem.

Chest imaging examination is crucial for the early detection of pulmonary tuberculosis (PTB) and monitoring whether treatment drugs are effective. There are imaging differences in the chest computed tomography (CT) scans of drug-sensitive tuberculosis (DS-TB) and DR-TB (2-4). When multiple CT signs of DR-PTB coexist, chest imaging examination can be used as a starting point for timely detection of suspected DR-TB patients and improve the efficiency of clinical diagnosis. In order to promote the effective implementation and promotion of imaging examination and standardized diagnosis of DR-TB, this consensus invited 36 Chinese national TB imaging experts to formulate an expert consensus on imaging diagnosis of DR-TB. This consensus is based on a review of the imaging literature on DR-PTB, combined with the methodological requirements of guidelines and standards for evidence-based medicine, comprehensive consideration of clinical practice, and the experience of specialist physicians to form the final recommendations for the imaging diagnosis of DR-PTB. The consensus was drawn to provide clinicians with a diagnostic basis, form the best decision-making scheme, and effectively improve the early diagnosis of DR-TB.

Overview

The main pathogen causing human TB is *Mycobacterium tuberculosis* (*M.tb*), which includes 4 types: human, bovine, African, and murine. More than 90% of the causative bacteria of human pulmonary TB is human-type *M.tb*. *M.tb* has the characteristics of pleomorphism, acid resistance, slow growth, and strong resistance (5). *M.tb* has complex bacterial components, mainly including lipids, proteins, and polysaccharides. Lipoids account for 50–60% and are related to tissue necrosis, caseous liquefaction, cavity occurrence, and TB allergic reactions in TB. The source of infection of *M.tb* is mainly sputum carrier particles, which is spread through droplets (6), and the susceptible population include those with low resistance, such as those with weak

self-resistance, human immunodeficiency virus (HIV) infection, and malnutrition (7). TB is an ancient disease, but its incidence remains high today. One of the main reasons is the prevalence of drug-resistant (DR) *M.tb*. The main reasons for drug resistance are as follows: (I) change of the structure and composition and the permeability of the cell wall, the drug permeability decreases, resulting in drug resistance; (II) mutations in genes encoding drug targets or enzyme genes related to drug activity on the *M.tb* genome produce degraded or inactivated enzymes, resulting in drug resistance (8); (III) bacteria exposed to low doses of drugs for a longer period of time can activate transporters and then overexpress them, leading to irreversible phenotypic drug resistance and eventually genetic drug resistance (9). The emergence of DR-PTB makes the diagnosis and treatment of TB more difficult, or even leads to treatment failure, resulting in the emergence of more chronic sources of infection that are difficult to cure. Therefore, in order to better control the TB epidemic, it is crucial to detect DR-TB early and provide timely and effective treatment.

Clinical manifestations

Similar to the clinical manifestations of DS-PTB, the main manifestations of DR-PTB are cough, sputum, low-grade fever, night sweats, weight loss, fatigue, loss of appetite, chest tightness and chest pain. In severe cases, blood in sputum or hemoptysis, wheezing and dyspnea may occur. The course of DR-TB is often protracted. The incidence of multiple cavities, bronchiectasis and large pulmonary consolidations is higher in DR-TB than in DS-TB, the lung damage is severer, and the structural damage of the lung is more common. Therefore, the respiratory system is more severely damaged (10). Some patients may experience extreme consumption such as long-term fever accompanied by malnutrition, anemia and hypoalbuminemia, and severe cases may even manifest as cachexia.

Clinical classification

With the development of therapeutic drugs and advances in drug resistance detection technology, the World Health Organization (WHO) continues to update its guidelines for the diagnosis and treatment of DR-TB, and revised the definition of DR-TB in October 2020, which took effect from January 2021. DR-TB can be divided into monodrug-resistant tuberculosis (MR-TB), RR-TB, MDR-TB, polydrug-resistant tuberculosis (PDR-TB), pre-extensive drug-resistant tuberculosis (pre-XDR-TB) and extensive drug-resistant tuberculosis (XDR-TB) (11,12). The above classification applies to all new and post-treatment DR-PTB, including pulmonary TB and extrapulmonary TB.

Main laboratory tests for DR-TB

Laboratory examinations include pathogenic examination, pathological and molecular pathological diagnosis, and immunological examination.

Etiology examination

Etiology examination includes *M.tb* smear microscope examination, *M.tb* culture and strain identification, and drug sensitivity test (DST). The detection method for DR *M.tb* is the same as that for DS-TB. Detection of the susceptibility of anti-TB drugs with isolation of culture-positive strains identified as *M.tb* complex is the gold standard for the diagnosis of DR-TB. By culture, the sensitivity of *M.tb* to a variety of first- and second-line anti-TB drugs can be determined, yet the disadvantages of the culture method are that is time-consuming, uncertain test results for some drugs such as pyrazinamide, and high demand for biological safety. The commonly used *M.tb* culture and DST methods include: *M.tb* solid culture and DST and *M.tb* liquid culture and DST (13). Points to be noted: (I) *Mycobacterium* culture: *Mycobacterium* culture should be performed on all samples of PTB patients. A positive culture and identification of *M.tb* can not only confirm the diagnosis, but also allow further DST. (II) Mycobacterial species identification: patients with PTB are prone to secondary or combined non-tuberculous mycobacteria (NTM) infections, and bacterial species identification is required to confirm the diagnosis. Species identification of clinical specimens or mycobacterial isolates can determine whether a patient has TB, nontuberculous mycobacteriosis, or co-infections. (III) *M.tb* DST: with the global resurgence of the TB epidemic, the proportion of DR-TB is increasing annually both for new patients or previously treated TB patients. DST should be routinely performed on TB patients to confirm drug resistance.

Pathological and molecular pathology diagnosis

The specific pathological changes of DR-TB have been a hot research topic in the pathology community. Unfortunately, no specific pathological differences between DR-TB and DS-TB have been found. Both can manifest 3

Table 1 Common *M.tb* resistance-related genes

Name of drug resistance	Related genes and mutation sites
Rifampicin	Codons 531, 526, and 516 of the rpoB gene. Most cases are co-resistant to isoniazide; codons 513, 526, and 531 can be cross resistant to rifampicin
Isoniazide	KatG, inhA, kasA and ahpC are mainly characterized by mutations in the coding region of the katG gene and the regulatory region of the inhA gene
Ethambutol	Mainly related to mutations in the embABC operon gene, with embB306, embB406, and embB497 mutations being the most common
Pyrazinamide	The relative hot spot mutation regions of the pncA gene are codons 3–17, 61–85 and 132–142
Streptomycin	The rpsL and rrs genes, codons 905 and 513 of the rpsL43 and rrs genes are the most common mutation sites
Fluoroquinolones	gThe yrA and gyrB genes, codons 90, 91, and 94 of gyrA, and codons 464 and 495 of gyrB are the most common

major pathological changes: exudative lesions, proliferative lesions and necrotic lesions. In the process of TB, affected by factors such as the virulence of *M.tb*, the amount of infecting bacteria, and the body's own immunity, the above 3 pathological changes often exist in a mixed manner. Different stages or different disease sites are mostly dominated by certain pathological changes and evolve into each other (14).

The characteristic histological manifestation of DR-TB is tubercles, which are mainly composed of epithelioid cells and Langhans giant cells. Caseous necrosis can be seen in the center of the nodules, and varying amounts of small lymphocytes and plasma cells can be seen around infiltration (15). Since the pathology of DR-TB is not substantially different from that of DS-TB, pathological specimens of suspected DR-TB patients can be tested for molecular DST or phenotypic DST, or next-generation sequencing (NGS) technology to confirm drug resistance as soon as possible.

With the promotion and popularization of clinical methods such as minimally invasive surgery and needle biopsy, the availability of sampled small tissues and punctured tissues is increasing; however, pathologists cannot diagnose TB by referring to gross specimens with the naked eye and typical histomorphological changes under the microscope. Higher requirements and greater challenges are put forward for pathological diagnosis. When seeing "atypical" pathological changes, the possibility of TB should still be considered.

Molecular pathological examination has become one of the diagnostic methods for DR-TB, mainly referring to the molecular biology drug susceptibility test of *M.tb* (referred to as "molecular DST") (16).

Mutations in DR-related gene sequences can cause *M.tb* to become resistant to anti-TB drugs. Common *M.tb* resistance-related genes are shown in *Table 1*. This type of method mainly judges whether the strain is resistant to the corresponding anti-TB drugs by detecting whether there is a mutation in the DR-related gene. Common detection techniques include real-time fluorescent quantitative polymerase chain reaction (qPCR), isothermal amplification, probe-reverse hybridization, probe-based melting curve and gene chip technology.

Immunological examination

Tuberculin skin test (TST) moderately positive or strongly positive, new tuberculin skin test (C-TST) positive, or gamma-interferon release test positive, interleukin 2 (IL-2) test positive, interferon-induced protein-10 (IP-10) messenger RNA (mRNA) transcription test positive, and *M.tb* antibody positive, can be used as auxiliary diagnostic criteria for TB. However, immunological techniques cannot distinguish DR-TB and DS-TB. Therefore, immunological examination has limited relevance in distinguishing DR-TB from DS-TB (17).

Imaging examination

The evidence level evaluation of evidence-based medicine in this consensus follows the principles of the grading of recommendations assessment development and evaluate (GRADE), and used the 2011 edition of Oxford Center for Evidence-Based Medicine Grading (OCEBM levels of evidence) as a supporting tool to perform evidence grading. Regarding the conversion of evidence into recommendations,

Table 2 GRADE level of evidence and grade of recommendation (18)

GRADE grading system	2011 Oxford Center for Evidence-based Medicine Evidence Classification
Level of evidence	
I	Systematic evaluation or meta-analysis of diagnostic tests designed based on cross-sectional studies (independent blind comparison with recognized gold standards)
II	Diagnostic tests designed for a single cross-sectional study (independent blind comparison with recognized gold standards)
III	Diagnostic tests designed for a single cross-sectional study (without independent blind comparison with recognized gold standards) or discontinuous studies
IV	Case-Control study
V	Mechanism-based reasoning or expert experience and consensus
Grade of recommendation	
Strong	Very confident. The true value is close to the estimated effect. Based on: high-quality research evidence supporting net benefits (e.g., advantages outweigh disadvantages); the research results have good consistency, with few or no exceptions; slight or no doubts about the quality of the research; and/or obtain the consent of the expert group members. Other recommendations based on high-quality evidence, including those discussed in the review and analysis of the guidelines, can also support strong recommendations
Medium	Moderate confidence in the estimated effect. Based on: good research evidence supporting net benefits (e.g., advantages outweigh disadvantages); the research results are consistent, with slight and/or few exceptions; slight or minor doubts about the quality of the research; and/or obtain the consent of the expert group members. Other recommendations based on medium-quality evidence with advantages outweighing disadvantages (including those discussed in the review and analysis of the guidelines) can also form medium recommendations
Weak	Confidence in the estimated value of the effect is weak, and this recommendation provides the best guidance currently available for clinical practice. Based on: limited research evidence supporting net benefits (e.g., advantages outweigh disadvantages); the research results are consistent, but there are important exceptions; There are important doubts about the quality of research; and/or obtain the consent of the expert group members. Other weak recommendations can also be formed based on limited evidence, including the review and analysis discussed in the guidelines

the expert group mainly followed the GRADE guidelines for grading recommendations, and made modifications to the recommendation grading in combination with the grading scheme of the American Society of Clinical Oncology (ASCO) guidelines (*Table 2*) (18). Finally, the recommendation strength is divided into 3 levels: strong recommendation, moderate recommendation and weak recommendation. A strong recommendation means that the panel has a high level of confidence that the recommendation reflects best clinical practice and should be adopted by most or all intended users. A moderate level of recommendation means that the expert group has a moderate level of confidence that the recommendation reflects the best clinical practice, and most target users will adopt the recommendation, but care should be taken in consideration of doctor-patient joint decision-making during implementation. A weak recommendation means that the expert group has certain confidence that the recommendation reflects the best clinical practice, but it should be applied conditionally to the target group, emphasizing the joint decision-making of doctors and patients.

Chest X-ray examination

Chest X-ray can be used as the first-line screening method for DR-PTB (level of evidence: III, strength of recommendation: strong), and is also a commonly used method for treatment efficacy evaluation (19) (level of evidence: IV, strength of recommendation: strong). Chest X-ray is of low cost and low radiation dose and has other advantages, but the diagnostic sensitivity and specificity are not optimal (20).

CT

CT is the main method for diagnosing DR-PTB (19)

(evidence level: IV, recommendation strength: strong). It is recommended to perform routine plain scans, and enhanced scan when necessary. CT can detect earlier PTB lesions than chest X-ray, and accurately assess the disease process, lesion activity, and complications (4).

CT has advantages in the diagnosis of lymph node morphology and enhancement features in differentiating TB from non-TB (21,22). CT can quantify pleural effusion, and multi-slice CT can make a more definite diagnosis of acute miliary TB. CT cannot only identify pulmonary consolidation, but also detect pulmonary cavitary lesions and accurately display the morphology of the cavity wall (21). "Tree-in-bud sign" is a typical manifestation of PTB, and 95% of cases show this sign on CT (23). Bronchiectasis and residual cavities are complications of PTB, and in 71–86% and 12–22% cases these lesions can be seen on CT, respectively (22). In addition, chest CT can show TB lesions in the spine, liver and spleen, which is helpful in the diagnosis of extrapulmonary TB (24).

CT provides an objective basis for evaluating the treatment efficacy for DR-TB. CT multi-planar reconstruction, especially coronal minimum density projection, can evaluate the entire large airway, further improve the accuracy of measuring airway stenosis, and provide a virtual roadmap for monitoring the dynamic response to treatment and precise surgical planning for lesion resection (25).

Other imaging examinations

Magnetic resonance imaging (MRI)

MRI can be used as a supplementary examination method for DR-PTB (evidence level: IV, strength of recommendation: medium). MRI shows excellent contrast resolution in showing lymph nodes, pleural abnormalities and caseous lesions. The sensitivity and specificity of MRI in detecting lymph nodes are comparable to those of CT. Lymph node TB and reactive lymphadenitis are further distinguished based on signal intensity and heterogeneity. Enhancement after enhancement indicates active lesions (26). However, MRI cannot detect lymph nodes smaller than 3 mm (4). MRI signal changes according to the stage of necrosis and whether mycobacteria are present in the necrosis. It is better than CT in qualitatively identifying lung consolidation, but it is difficult to detect subtle manifestations such as ground-glass density shadows in the lungs. For the detection of a small amount of pleural effusion that cannot be shown by CT, MRI is superior to CT (27).

Positron emission tomography (PET)/CT

PET/CT is a supplementary examination method for DR-TB (level of evidence: IV, strength of recommendation: weak). PET/CT can distinguish active and inactive PTB and assist in evaluating treatment effects. However, its diagnostic specificity for solitary pulmonary nodules is low, making it difficult to differentiate TB from malignancies (28).

Chest ultrasound

Chest ultrasound is a portable, non-invasive, and supplementary examination method for the evaluation of intrathoracic lesions of DR-PTB (21) (level of evidence: IV, strength of recommendation: weak). Some 31–83% of patients may show abnormal ultrasound findings, including lung consolidation, pleural effusion, or lymphadenopathy. Another advantage is for the evaluation of extrapulmonary TB, including evaluation of peritoneal effusions, hepatic micro-abscesses, or abdominal lymph nodes.

Artificial intelligence imaging

In March 2020, WHO approved the use of computer-aided detection (CAD) software as an alternative to human interpretation of chest radiographs for TB screening and triage in susceptible people over 15 years old (29) (level of evidence: IV, strength of recommendation: weak). A scoring system to predict the likelihood of DS or DR TB is cost-effective and user-friendly for use in low- and middle-income countries with high TB burden and insufficient number of radiologists and may meet minimum acceptable requirements for TB triage with acceptable sensitivity and specificity.

Imaging diagnosis

DR and CT imaging manifestations

DR-TB is different from DS-TB in lesion distributions. DR-TB is more likely to cause lung tissue damage and has a wider distribution of lesions. It is not limited to the sites where PTB is susceptible. DR-TB can also be found in non-prevalent sites of PTB, such as the middle lobe of right lung, lingual segment of the left lung, and basal segments of the lower lobes (evidence level: IV, recommendation strength: weak).

Both DR-TB and DS-TB images can have nodules, pulmonary infiltrates, consolidation, cavities, damaged lungs, ground glass opacity (GGO), calcification, fibrosis,

bronchiectasis, bronchial wall thickening, atelectasis, pleural effusion and thickening, lymphadenopathy, and other manifestations (30-37). However, the prevalence of pulmonary nodules, consolidations and cavities is higher in DR-TB (33-36). Some researchers believe that pulmonary nodules are the only manifestation on chest radiography that distinguishes MDR-TB from DS-TB (37) (level of evidence: IV, recommendation strength: weak). Compared with MDR-TB, patients with DS-TB have more obvious infiltrative lesions and mostly occur in the upper lungs. Chronic manifestations such as mediastinal shift, upward hilar shift, pleural effusion, and pleural thickening are more common in MDR-TB (2,34,38) (level of evidence: IV, strength of recommendation: strong).

Imaging signs related to cavities are of the most importance for diagnosing MDR-PTB (2,4,35,39,40). Almost all articles have reported that the biggest difference between DR-PTB and DS-PTB lies in the size, number and thickness of cavities. When comparing DR-PTB and DS-PTB patients with cavities, the cavities of DR-PTB have a higher number and are more likely to be thick-walled and more widely distributed. Damaged lungs are more prevalent in MDR-PTB (level of evidence: IV, strength of recommendation: strong).

(I) Number of cavities: 68.3% of MDR-TB has multiple cavities (313/458). MDR-TB has 2–7 cavities, with an average of 3.1 cavities. XDR-TB has more cavities, with an average of 4.1 cavities. The number of cavities in DS-TB is 1–3, with an average of 1.4. The number of cavities ≥3 has great value for the diagnosis of MDR-TB (evidence level: IV, recommendation strength: strong).

(II) Inner diameter of cavities: compared with DS-TB, the inner diameter of MDR-TB cavities is larger, with 83.7% (77/92) having an inner diameter >30 mm, and the average inner diameter of cavities is 29 mm; the average inner diameter of XDR-TB is 36 mm, and the cavities of XDR-TB are larger (level of evidence: IV, strength of recommendation: strong).

(III) Cavity wall thickness: thick-walled cavities are more common in MDR-TB than in DS-TB (evidence level: IV, recommendation strength: strong). The occurrence of thick-walled cavities in MDR-TB can reach 62.3% (264/424). The cavity wall thickness can reach 8 mm, and XDR-TB cavity walls are even thicker, with an average of 11 mm.

(IV) Distribution of cavities: compared with DS-TB, MDR-TB cavities are more widely distributed and more likely to appear in multiple lobes, accounting for 62.9% (222/353) of all cavities.

(V) Cavity type: MDS-TB has more variable cavity types than DS-TB. For MDR-TB cases, cavitation occurs more frequently in consolidations, nodules and masses, accounting for more than 50% of cavitations (41).

In cases where there are ≥3 cavities in a patient, cavities have thick-wall and lesions distributed in more than 3 lobes, these are important imaging basis for the diagnosis of DR-PTB (evidence level: IV, recommendation strength: strong).

Depending on the type of drug resistance, duration of disease, and treatment status of DR-TB patients, the distribution, extent, size, and incidence of imaging findings are also different.

Imaging manifestations of MR-TB (including RR-TB)

The imaging manifestations of MR and RR-PTB have certain similarities. Therefore, the imaging manifestations of MR described here include the imaging manifestations of RR-PTB. Although most experts believe that the imaging differences between MR-TB and DS-TB are small, there are still certain differences between the 2 entities according to existing literature.

MR-PTB are more widely distributed than DS-PTB, and most are distributed in more than three lobes of the lung. In addition to the occurrence of MR-TB in the susceptible site of TB, MR-PTB is also more likely to involve the non-susceptible site of TB, such as the right middle lobe and the basal segments of the lower lobes (42-44). Compared with DS-TB, MR-PTB is more prone to lung consolidation, cavitation, bronchial thickening, lymphadenopathy, and pleural effusion (42-44). However, about 58% (23/40) of the cavities in MR-PTB are nodular cavities, and the cavities are relatively localized, mainly a single cavity in a single lobe (44) (*Figure 1*).

In view of the paucity of imaging-related literature on MR-TB and the limited study sample size, the above-mentioned manifestations may not be generalizable. Therefore, the strength of the current recommendation for this aspect is still insufficient.

Imaging manifestations of MDR-TB (including PDR-TB)

Compared with DS-TB, the CT manifestations of MDR-TB are more complex. MDR-TB patients have a higher incidence of lung parenchymal damage, the lesions are more widely distributed, and multi-lobar lung segments are

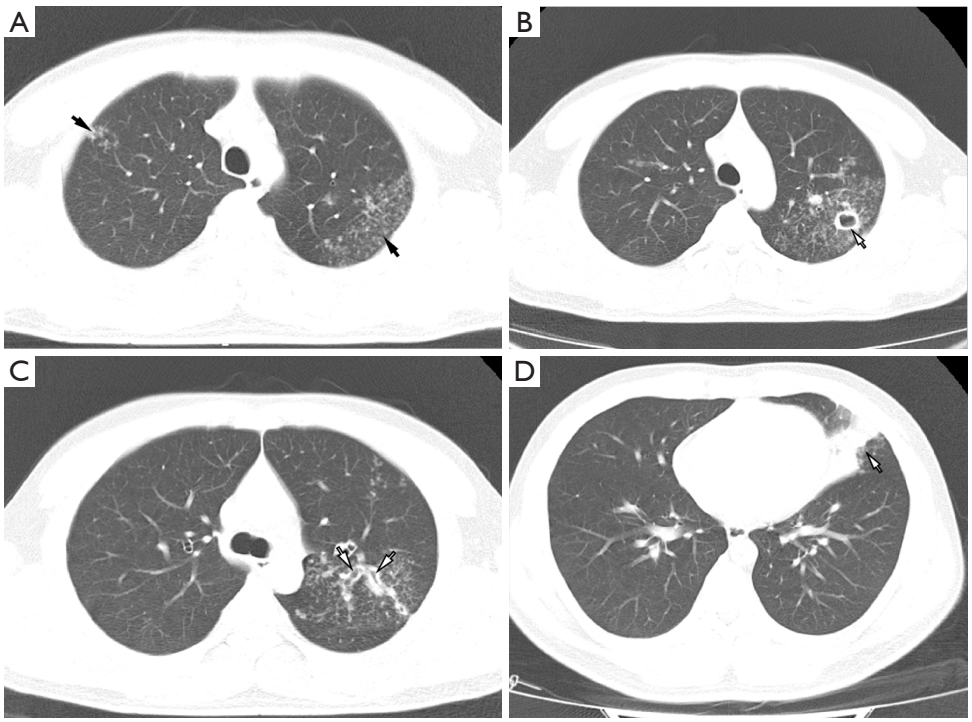

Figure 1 CT of a case of rifampicin-resistant pulmonary tuberculosis (male, 20 years old). (A) Scattered centrilobular nodules and tree-in-bud signs are seen in the apical and apicoposterior segments of the upper lobe of both lungs, with blurred borders (black arrow); (B) a thick-walled cavity is seen in the posterior segment of the upper lobe of the left lung (white arrow), and satellite lesions are seen surrounding the cavity; (C) bronchiectasis and wall thickening are seen in the apicoposterior segment of the upper lobe of the left lung (white arrow), and multiple centrilobular nodules are seen around it. (D) Flake consolidation is seen in the lower lingual segment of the upper lobe of the left lung (white arrow). CT, computed tomography.

more likely to be observed (4,45-47) (*Figure 2*). In MDR-TB, in 80–93% of cases, both lungs have lesions (31,48,49), in 86.1–91% of cases, the lesions are distributed in 3 or more lung lobes, and in 61.3% of cases, there is whole lobe involvement (48,50). Compared with DS-TB, MDR-TB is more likely to occur in non-susceptible sites such as the anterior segment of the upper lobe, lingual segment of the middle lobe, and basal segments of the lower lobes (48,50). These observations may be related to the fact that MDR-TB is mostly acquired DR, the course of the disease is protracted, and the lesions continue to spread in the lungs.

MDR-TB has a variety of CT manifestations, including exudation, consolidation, cavity, nodule, cord, calcification, bronchiectasis and stenosis, pleural thickening, pleural effusion, and lymph node enlargement (*Figure 2*). Among them, cavitation is the CT finding with the most diagnostic value for MDR-TB (2,4,38-40,45-48,50). The incidence of cavitation in DS-TB patients is only about 20–40% (2,51), whereas the incidence of cavitation in MDR-TB is relatively high. Regardless of whether for new MDR-TB or re-treatment MDR-TB, there is a high incidence of cavitation (2,4,38-40,45-48,50). The number of cavities in MDR-TB is related to the length of medical history. The number of cavities in MDR-TB and DS-TB patients with a history of TB <1 month is basically similar, whereas the number of cavities in MDR-TB patients with a medical history of more than 1 month is more than that of DS-TB patients (52). Nearly 70% of re-treatment MDR-TB patients will develop multiple cavities, with an average of 70–85% and even up to 100% (31). Multiple cavities are of diagnostic value for MDR-TB; the most valuable CT finding for diagnosing MDR-TB is a number of cavities is greater than 3 or a diameter of cavities is greater than 30 mm (2,4,38-40,47). The diameter of the cavity in MDR-TB is significantly higher than that in DS-TB patients, reaching an average of 47 mm (48). The incidence of thick-walled cavities and damaged lungs is also higher in MDR-TB than in DS-TB (2,44,46,47,53). Thick-walled cavities have insufficient blood

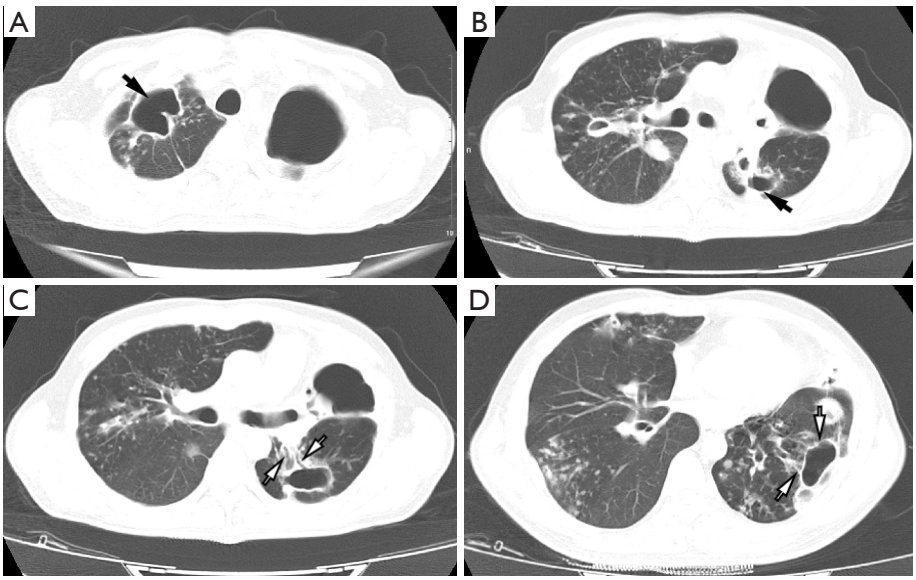

Figure 2 CT of a case of MDR-TB (male, 37 years old). There are multiple cavities of different sizes and irregular shapes in both lungs (A-D) (black arrows, white arrows). The walls of the cavities are unevenly thick. Nodules and cord-like satellite lesions are seen around the cavities (A,B,D). The cavities in the upper lobe of left lung merged to form the damaged lung (A-C). There are scattered small patchy shadows, centrilobular nodules, and tree-in-bud signs in both lungs, with irregular shapes (A-D). There are multiple bronchiectasis and wall thickening in both lungs, and some are cavity draining bronchi (C,D; white arrows). CT, computed tomography; MDR-TB, multidrug-resistant tuberculosis.

supply, and the low-concentration anti-TB drugs inside the cavities cannot effectively kill TB bacteria, which is the main reason why MDR-TB cavities are difficult to close and the risk of drug resistance increases (2,44).

In addition to differences in the size and number of cavities, the prevalence of caseous pneumonia, damaged lungs, tree-in-bud sign, consolidation, nodules and centrilobular nodules, bronchiectasis, bronchial stenosis, pleural thickening, thoracic collapse and mediastinal shift, and pericardial thickening, are all significantly higher in MDR-TB than in DS-TB (2,50,52,53).

In addition, the incidences of parenchymal involvement of bilateral lungs, multiple cavities, bronchiectasis, cavities, nodules, or masses are higher in new MDR-PTB than those in DS-PTB, and the lesion extent are larger in new MDR-PTB (50,52,54). Calcification of intrapulmonary lesions and calcified lymph nodes are more common in DR-TB (3). Patients with new MDR-TB have a higher incidence of cavities, bronchial wall thickening, and consolidation than those with DS-TB (42). The cavities in re-treatment MDR-TB patients have wider range, with a higher cavity number and larger cavities than those in new MDR-PTB patients (*Figure 2*). At the same time, the incidence of cavity wall calcification, lung consolidation, damaged lungs, emphysema, calcification, and bronchiectasis (*Figure 2C,2D*) is higher in post-treatment MDR-TB patients than that new MDR-TB patients (50,55), which may be related to the longer disease course (52).

Although MDR-TB has certain features in chest CT manifestations, its overall imaging manifestations are not intrinsically different from those of DS-TB patients (2,38,46). Both can manifest as wide lesion distribution, bronchial dissemination, multiple cavities, damaged lungs, pleural thickening, and bronchiectasis, only that these changes have a higher incidence in MDR-TB patients.

When the maximum diameter of the cavity is ≥30 mm, the number of cavities is ≥3, and the areas where the cavity exists is ≥3 lobes, these features are related to MDR-PTB. If there are large/extensive lesions in both lungs and chronic manifestations at the same time, MDR-TB should be highly suspected (evidence level: IV, recommendation strength: strong).

XDR-TB/pre-XDR-TB imaging appearance

XDR-TB/pre-XDR-TB patients are more difficult to treat than MDR-TB patients, have poorer drug efficacy, longer

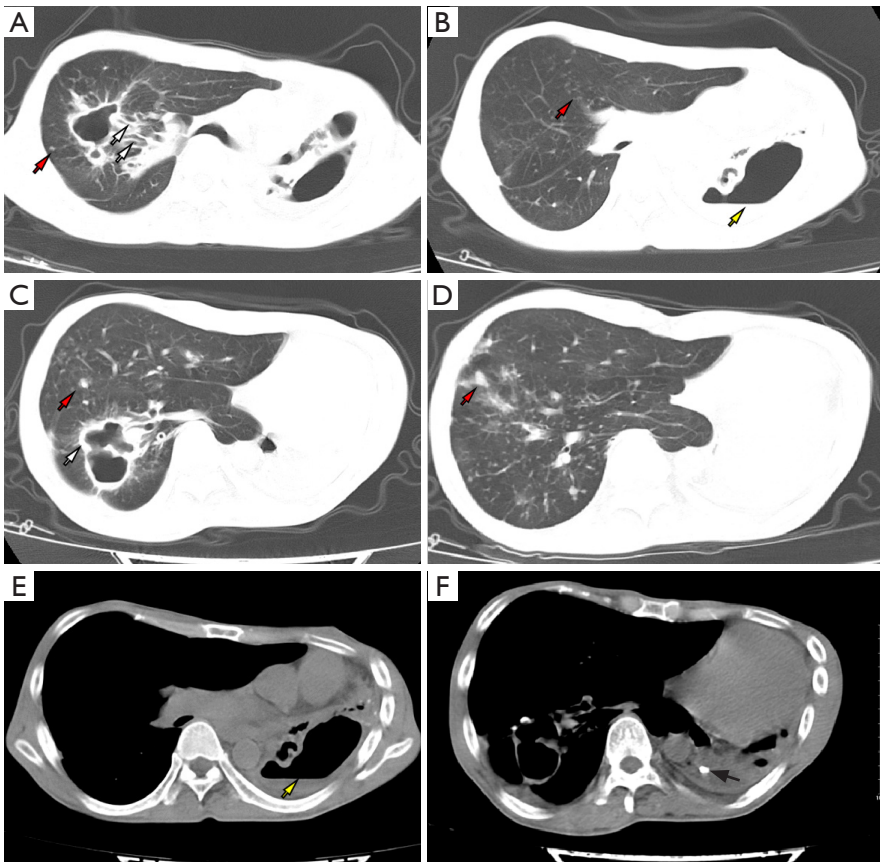

Figure 3 CT of a cases of pre-extensively drug-resistant tuberculosis (male, 36 years old). The left thoracic cavity is partially collapsed, the mediastinum shifted to the left (A-F). Multiple thick-walled cavities in the right lung, thickened and dilated draining bronchi are seen in the proximal end (A,C) (white arrows). The left lung is damaged, and an air-fluid level is seen in the damaged cavity (B,E) (yellow arrow). Multiple small nodules, cords, and tree-in-bud signs are seen in the right lung (A-D) (red arrows). Lesions seen in the right lung and nodular calcification in the left pleura (F) (black arrow). Bilateral pleural thickening, small amount of wrapped effusion in the left thoracic cavity (F). CT, computed tomography.

disease course, and more severe lung tissue structural damage (47). In addition to the manifestations of MDR-TB, XDR-TB/pre-XDR-TB lesions often involve more than 3 lobes of the lungs, and are more likely to cause multiple cavities, damaged lungs, and extensive airway dissemination and pulmonary consolidation. XDR-TB/pre-XDR-TB has thicker walls, higher numbers, and larger cavities than MDR-TB (2,47) (*Figure 3*). During the course of non-effective anti-TB treatment, XDR-TB/pre-XDR-TB intrapulmonary disseminated lesions continue to increase, the cavities enlarge, cavity numbers increase, and the cavity closure rate is low, reflecting the poor efficacy of XDR-TB/pre-XDR-TB treatment. The lesions are characterized by progressive deterioration. XDR-TB/pre-XDR-TB has more types of DR than MDR-TB, the resistance to anti-TB drugs is more severe, and the lesions are more widely distributed in the lungs, which can cause multiple dissemination in the lungs and cause protracted, progressive lesions. The degree of lung parenchymal damage in XDR-TB/pre-XDR-TB is higher than those in MDR-PTB patients, and the number of damaged lung segments involved is also more extensive than in DS-TB (56).

The high incidence of cavities and multiple cavities are important characteristics of XDR-TB/pre-XDR-TB (57). The prevalence of cavities in XDR-TB/pre-XDR-TB can reach 85%, which is higher than that of MDR-TB patients. The thickened cavity wall acts as a barrier to the entry of anti-TB drugs into the cavity. In addition, the elevated concentration of *M.tb* in the cavity and the insufficient blood concentration in the cavity increase the risk of *M.tb*

evolving into a DR strain (41,58).

Cavity lesions which spread to the lungs through the bronchus can cause caseous necrosis, tissue dissolution, and discharge, and subsequent formation of new cavities. The original cavities can continue to increase and merge with other lesions, damaging the lungs or further aggravating existing damage to the lungs. The increased number of cavities can easily cause bronchial dissemination and thus form a vicious cycle. This is one of the reasons why the incidences of cavities and disseminated lesions in XDR-TB/pre-XDR-TB patients are higher than those in MDR-TB patients. Among cases with cavities, the extent and size of cavities and intrapulmonary disseminated lesions in XDR-TB/pre-XDR-TB patients are greater than those in MDR-TB patients (57).

When CT shows multiple cavities, thick-walled cavities, extensive lung damage and bronchial dissemination, the possibility of XDR-TB/pre-XDR-TB should be considered.

Other imaging manifestations (MRI, PET/CT)

MRI manifestations

MRI does not have much advantage over CT in diagnosing DR-TB, but it is better than CT in reflecting the pathological characteristics of TB and can reflect different stages of TB (59-62). MRI is more sensitive for detecting caseous necrosis, liquefaction, active cavitation, lymph node and pleural changes (63). PTB has various signals on T2-weighted imaging (T2WI). On T2WI, hyperplastic granuloma shows high signal, caseous necrosis shows low signal, and liquefaction necrosis and exudative lesions show high signal (62). The most valuable sign of MRI in diagnosing PTB is T2WI low signal. When PTB contains more lipids, it may show slightly high signal on T1WI. T2WI signal changes can also be used to evaluate the TB activity and treatment efficacy of PTB (62).

PET/CT performance

Both MDR-TB and DS-TB can show high radioactivity uptake in ^{18}F fluorodeoxyglucose (^{18}F-FDG) PET/CT images, and whether the TB case is DR cannot be determined based on their maximum standardized uptake value (SUV_{max}) values. The average SUV_{max} of PTB is 6.63±4.82. The lesion SUV_{max} 2.5 is the critical value between active and inactive PTB, and inactive PTB is mostly below 2.0 (64,65). Although PET/CT is not the main examination method for diagnosing MDR-TB, it is useful for bacteria-negative MDR-TB patients with a long course of TB, those with a lack of typical clinical symptoms, those with less lesion activities on CT, those with proliferative fibrosis and other chronic changes. Lesion activity can be determined by SUV_{max} value (64).

Imaging manifestations of special types of DR-TB

Imaging manifestations of DR-PTB in children

The culture positivity rate of specimens from children with PTB is low (66,67), and the process from the onset of clinical symptoms to diagnosis is long, so early evaluation by imaging plays an important role. At present, there are few Chinese and international literature reports on the imaging manifestations of DR-PTB in children. This article synthesizes the relevant literatures on the imaging manifestations of DR-PTB and DS-PTB in children. The pediatric patients were grouped and discussed according to the age classification in the *Global tuberculosis report 2018* (less than 5 years old group and 5–14 years old group).

(I) Imaging features of DR-PTB in children less than 5 years old

Compared with DS-PTB in children of the same age group, DR children in this age group have more extensive distribution of pulmonary lesions, and bilateral lungs are often involved (*Figure 4*). The most common imaging manifestations are multiple nodules (including miliary nodules), followed by pulmonary consolidation, with a low incidence of cavitation (68,69). Tree-in-bud sign and calcification are rare. Hilar and mediastinal lymph node enlargement is common, but CT signs of bronchial TB such as bronchial stenosis, thickened tube wall, and unsmooth inner wall are rare (68), and the incidence rate is lower than the incidence rate of bronchial tuberculosis in children with DS-PTB (70,71). The incidence of pleural effusion, pleural thickening is low (68,69), and it is often accompanied by severe extrapulmonary TB, of which intracranial TB is the most common. The incidence of extrapulmonary TB such as intracranial TB in DR children is higher than that in children with DS-PTB (72,73).

(II) Imaging features of DR-TB in children aged 5 to 14 years

Compared with DS-TB children of the same age group, the incidence of DR-TB lesions involving bilateral lungs is higher (*Figure 5*). The main manifestations are multiple nodules, patchy shadows, pulmonary consolidation, hilar and mediastinal lymph node enlargement. The incidence of cavities in older children (5–14 years old) with DR-TB is higher than that in children less than 5 years old with DR-TB, but is similar to that of DS-TB in children of the same age (68). Tree-in-bud sign is common and

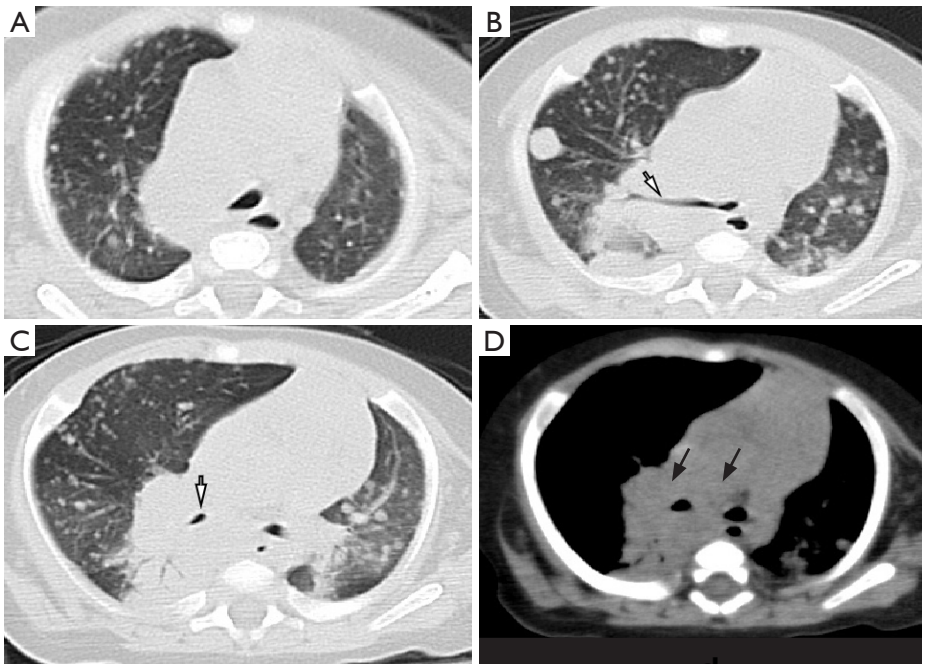

Figure 4 CT of a case of MDR (isoniazid, rifampicin, streptomycin) PTB (male, 5 months old). Widely distributed nodules of different sizes and multiple consolidation shadows in both lungs, uneven density, parts of the edges are unclear (A-C). (D) Mediastinum and multiple hilar lymphadenopathy (black arrows). Right main bronchus, right upper pulmonary bronchus, and middle bronchi are compressed and narrowed (white arrow). CT, computed tomography; MDR, multidrug-resistant; PTB, pulmonary tuberculosis.

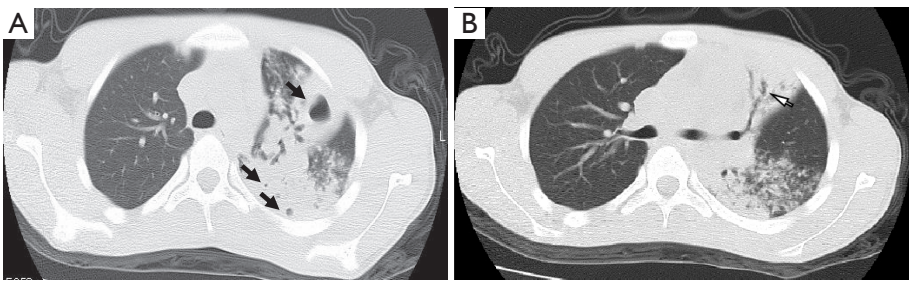

Figure 5 CT of a case of drug-resistant (isoniazid, moxifloxacin) pulmonary tuberculosis (male, 13 years old). (A) Multiple nodules, patches, and flaky consolidation shadows are seen in the apicoposterior segments of the left upper lobe and the dorsal segment of the lower left lobe with uneven density and unclear edges; and multiple wall-less cavities (black arrows) are seen inside the consolidation shadow; (B) the bronchus of the left upper lung is slightly narrowed, and the distal end is irregularly dilated (white arrow). CT, computed tomography.

calcification is rare. The incidence of bronchial TB is higher in DR-TB than in DS-TB (70). Pleural thickening is common, but the incidence of pleural effusion is low (68), which is much lower than the incidence of tuberculous pleural effusion in children with DS-PTB (73,74).

Imaging manifestations of DR-PTB in the elderly

The DR rate of post-treatment PTB in the elderly is higher than that of newly diagnosed patients with TB (75). The course of the disease is long and the lung lesions are extensive (76). Lesions involving more than 3 lung fields are significantly more common than those among young and middle-aged patients (77). Caseous lesions and cavities are more common (78). The incidence of tuberculous pleurisy and tracheobronchial TB is high (79,80). Lung damages are more common among re-treatment patients than among new patients. Long-term chronic disease causes pulmonary fibrosis, formation of lung cavities, and bronchiectasis and bronchostenosis twisting, which

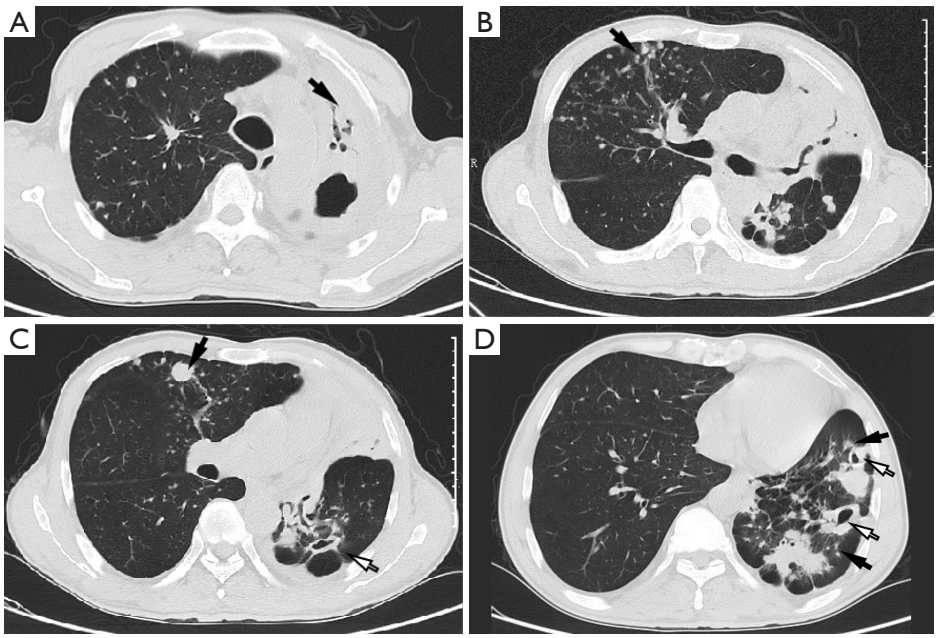

Figure 6 CT of an elderly patient with DR-TB (male, 60 years old). The lesions are widely distributed in both lungs, with proliferative nodules distributed in multiple lobes and the "tree-in-bud sign" (black arrow of B) seen (A-D). The upper lobe of the left lung is damaged, reduced in size, and presents as a large consolidation shadow (black arrow of A) (A-C), with multiple small and large wall-less cavities and dilated and twisted bronchial shadows (A-C). The left lower lobe bronchus is narrowed and twisted, and the lung structure has altered (white arrow) (C). There are multiple thick-walled cavities (white arrows) in the left lower lobe of the lung, with smooth inner walls and less smooth outer walls, and surrounding satellite foci seen (black arrows) (B-D). Left lower lobe emphysema with mediastinal shift to the left (B-D). Left pleural thickening and adhesions (C,D). CT, computed tomography; DR-TB, drug-resistant pulmonary tuberculosis.

alter the lung structure (76) (*Figure 6*). DR-PTB in the elderly is often accompanied by underlying diseases such as chronic bronchitis, emphysema, bullae, and a small number of patients may have pneumothorax. It is more common to develop secondary pulmonary infection with other MDR pathogenic bacteria (81,82), and the prognosis is poorer.

Imaging manifestations of acquired immunodeficiency syndrome (AIDS) co-existing with DR-PTB

AIDS patients' immune function is impaired or defective and they often co-exist with opportunistic infections. PTB is a common opportunistic infection in AIDS patients. The global TB report released by WHO in 2022 pointed out that an estimated 187,000 AIDS patients worldwide would die from TB in 2021 (1). In the early stage of AIDS, the chest imaging features of patients infected with *M.tb* are not different from those of other patients with DS-PTB. However, in the middle and late stages of AIDS, as the count of $CD4^+$ T lymphocytes continues to decrease, the imaging manifestations become increasingly atypical, and the lesions have diverse shapes, involving multiple lobes and lung segments, and usually appear as atypical infiltrates and miliary lesions. Mediastinal lymph node enlargement and pleural effusion are more common, whereas cavitation, nodules, old fibrous lesions and lymph node calcification are relatively less common (83,84) (*Figure 7*).

Differential diagnosis of PR-PTB

Differentiation from non-tuberculous mycobacteriosis

NTM refers to mycobacteria other than *M.tb* complex and *Mycobacterium leprae*. The bacteria mainly invade the lungs. There are certain similarities with DR-TB, but both also have their own characteristics (19,48,85-88).

Radiologically, (I) NTM lung disease is more likely to cause thin-walled cavities (the prevalence is about 33%) (89). NTM infection firstly induce the formation of granulomas in the terminal bronchioles, and then spread through the bronchi, and the airway muscle layer is destroyed. The

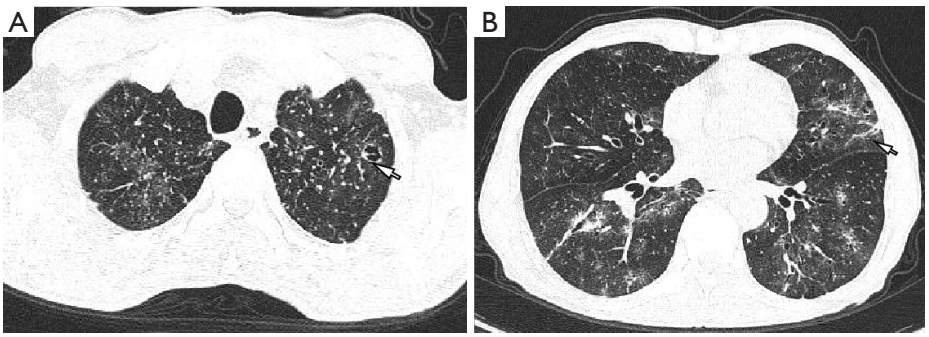

Figure 7 CT of a patient with HIV and DR-TB (male, 68 years old). Diffuse small nodules and miliary nodules are seen in both lungs, some are randomly distributed or distributed along the bronchi (A,B), with uneven density and some with unclear boundaries. Scattered patchy and nodular GGOs in both lungs with blurred borders (A,B). A small thin-walled cavity (white arrow) is seen in the upper lobe of the left lung with streaks seen inside (A). The dilated bronchi are seen in both lungs, some with thickened walls and some lumens are twisted and irregular (white arrow). Subpleural interlobular septa of both lungs are thickened and blurred (B). CT, computed tomography; HIV, human immunodeficiency virus; DR-TB, drug-resistant tuberculosis; GGOs, ground glass opacities.

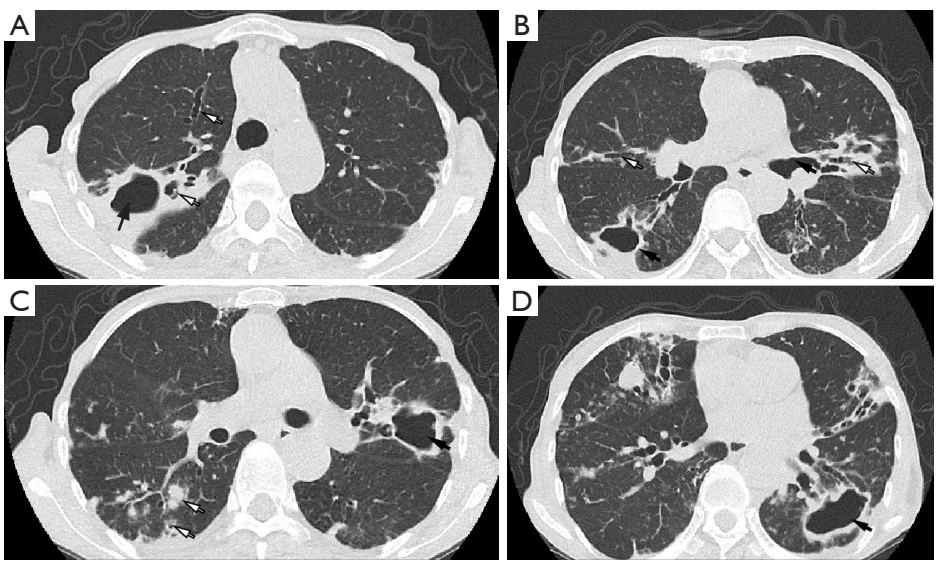

Figure 8 CT of a case of NTM (male, 68 years old). (A-D) Multiple sites of severe bronchiectasis in both lungs. Multiple thick-walled cavities are found in both lungs, and the inner walls of the cavities are smooth, and the cavities have a subpleural distribution. (A) An air-fluid level is seen in the cavity (black arrow) in the right upper lobe; (B) multiple bronchiectasis seen in the right middle lung lobe and left lingual segment (white arrow), cavity seen in the right upper lobe (black arrow); (C) the walls of the dilated bronchi are thickened, and multiple nodules can be seen around them, and lobular small central nodules (white arrows) can be seen in the lower lobe of the right lung; (D) dilated draining bronchi on the hilar side of the cavity (black arrow). CT, computed tomography; NTM, non-tuberculous mycobacteria.

airway becomes narrowed or even blocked, resulting in thin-walled cavities (85) (*Figure 8*). Thick-walled cavities appear in patients with PTB, whereas thin-walled cavities in NTM lung disease are often surrounded by satellite lesions distributed in segments or lobes (90). (II) NTM lung disease is more likely to cause bronchiectasis, which is common in the lingual lobe of the left lung and the middle lobe of the right lung (88) (*Figure 8*). Some studies have pointed out that bronchiectasis is a susceptibility factor to NTM infection (91). There is no significant difference in bronchiectasis and bronchiolar wall thickening between NTM and those due to PTB, except that MDR-PTB more

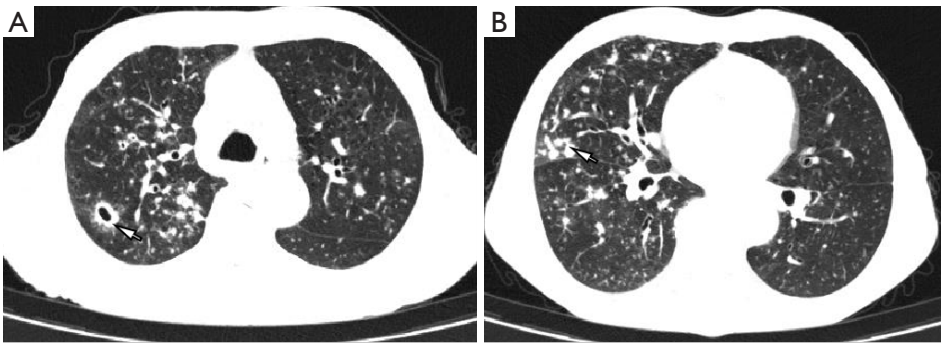

Figure 9 CT of a case of airway invasive pulmonary aspergillosis (male, 70 years old). (A) A thick-walled cavity and bronchial wall thickenings in the upper lobe of the right lung. The inner wall of the cavity is smooth, and halo signs (white arrow) are seen. Multiple nodules in both lungs are seen, some of which are distributed along the bronchi with blurred boundaries. (B) Impacted bronchi with dilatation (white arrow) are seen under the pleura in the upper lobe of the right lung. GGO shadows are seen around these lesions. CT, computed tomography; GGO, ground glass opacity.

often involves the upper lobes, whereas NTM lung disease more commonly involves the middle and lower lobes (92). (III) NTM lung disease usually manifests as centrilobular nodules, and CT images show clustered micronodules, most of which are less than 5 mm in size, and parenchymal infiltration lesions rarely occur around the bronchi and bronchioles (*Figure 8*), thus nodules and bronchiectasis are the typical imaging findings of NTM (88). DR-PTB often manifests as dissemination lesion in peribronchus or other lung fields, and acinar nodules more likely to appear. (IV) DR-PTB more likely involves the adjacent pleura than non-tuberculosis mycobacteria, and the damage to lung tissue is more severe. In NTM lung disease, lung consolidation and atelectasis occur only when the large airways are involved, but the occurrence is low (93). (V) The main sites of NTM lung disease are the middle lobe of the right lung and the lingual segment of the upper lobe of the left lung. However, there is no significant difference in the extent of nodule involvement between the 2 diseases. It is sometimes difficult to distinguish DR-PTB from NTM clinically, but the differential diagnosis can be made through laboratory tests and imaging features (94). When the identification is difficult, diagnosis should be made with the help of immunological tests, sputum culture bacteriology, and DST, and it is very important to administer a targeted treatment plan according to the testing result.

Differentiation from pulmonary mycosis

The imaging manifestations of DR-PTB are complex and diverse, often involving multiple lung lobes, multiple nodules and cavities, and prone to intrapulmonary dissemination (95). The incidence of lobar consolidation and atelectasis is relatively high, and even the lungs are damaged, and extrapulmonary lesions such as pleural effusion and mediastinal lymphadenopathy are prone to occur (47). The main differential diagnosis for DR-PTB includes pulmonary mycoses such as pulmonary aspergillosis and pulmonary cryptococcosis (PC).

Pulmonary aspergillosis

Airway invasive pulmonary aspergillosis

Airway invasive pulmonary aspergillosis is pathologically characterized by hyphae invading or growing along the bronchial mucosa, manifesting as bronchial granuloma and invasive tracheobronchitis. The imaging manifestations include small nodules and short linear shadows distributed along the bronchi, forming the tree-in-bud sign (96). Thickening of the bronchial wall, narrowing of the bronchial lumen, bronchial dilation and deformation, and destruction of bronchial cartilage can be seen. When the proximal bronchus is blocked by hyphae, there are fewer surrounding proliferative foci with blurred edges, yet there are more GGOs (97) (*Figure 9*). The tree-in-bud sign is also common in DR-PTB, DR-PTB has relatively more proliferation foci with and clear edges, while GGO shadows are less common.

Vasoinvasive pulmonary aspergillosis

The pathological mechanism of vasoinvasive pulmonary aspergillosis is that hyphae invade and block small arteries, causing local pulmonary infarction and lung parenchymal involvement. Early manifestations include single or multiple

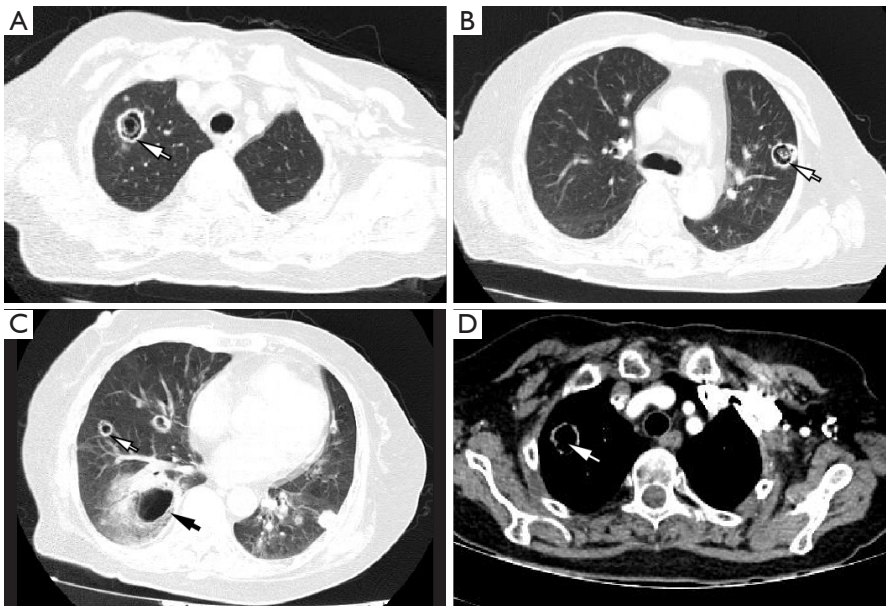

Figure 10 CT of diabetic patient with chronic cavitary pulmonary aspergillosis (female, 73 years old). (A-C) There are multiple thick-walled cavities and nodular shadows of different sizes in both lungs. (A) There is a cavity in the upper lobe of the right lung, with annular slightly low-density shadows seen inside. Small nodules and a few patchy GGO shadows are seen around this cavity (white arrow); (B) irregular air-containing nodular shadows (white arrow) are seen inside the cavity in the upper lobe of the left lung; (C) there are multiple cavities here (white arrow, black arrow), with the larger one located in the right lower lung (black arrow), its inner wall is smooth, and halo sign is seen around the cavity (black arrow); (D) the cavity wall is slightly enhanced on the enhanced scan (white arrow). CT, computed tomography; GGO, ground glass opacity.

nodules and consolidation shadows, often accompanied by a halo sign (98). Halo sign is less common among DR-PTB pulmonary nodules. As the disease progresses, necrosis begins to appear in the consolidation area of invasive pulmonary aspergillus lesions, and parts of the necrotic material are discharged through the bronchi, causing the air crescent sign. Later in the disease course, cavities will appear, and there are often contents in the cavities, namely mycelia (98). The cavities in the lungs of DR-PTB are mostly thick-walled cavities, and there is generally no inner content in the cavities. In addition, invasive pulmonary aspergillosis progresses quickly, and lung lesions can change significantly within a few days, whereas DR-PTB has a longer course and is more likely to have extrapulmonary manifestations than invasive pulmonary aspergillosis (96).

Chronic cavitary pulmonary aspergillosis (CCPA)

CCPA is often secondary to old PTB, diabetes, and other diseases. It usually presents as 1 or more cavities, which can be thin- or thick-walled (99). According to the different development stages of aspergillus, CCPA will show different CT signs, which are divided into 5 categories: typical aspergilloma, mural nodule, cavity wall thickening, partial soft tissue filling, and complete soft tissue filling. On enhanced scan, these inner contents are not enhanced (98). However, the imaging manifestations of DR-PTB are mainly the signs of the active phase, manifested as multiple cavities and disseminated lesions in the lungs, and the cavities generally do not contain inner contents. In addition, the incidence of lobar consolidation and atelectasis in DR-PTB is high, and it is common to show damaged lungs, whereas these signs are rarely seen in CCPA (*Figure 10*).

PC

PC has various manifestations, with nodules and masses being the most common. PC mostly occurs in the subpleural and peripheral lung zones, with a wide base connected to the pleura. Lobulation signs and long spicules can be seen. Halo sign can be seen at lesion's edge, whereas calcification is rare. Cavity within the lesion is relatively uncommon and cavities are generally thick-walled, with uniform and smooth walls and without surrounding satellite

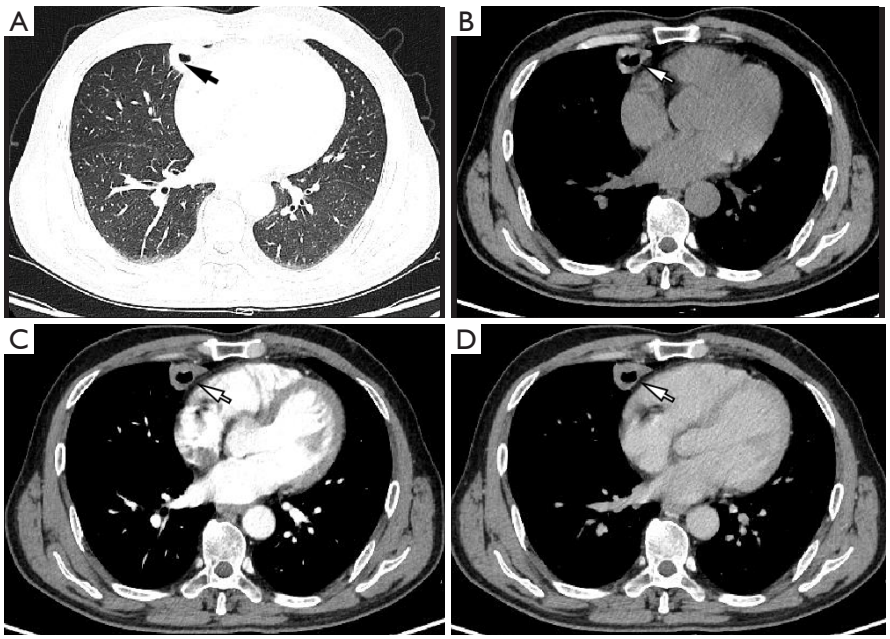

Figure 11 CT of a case of pulmonary cryptococcosis (male, 57 years old). (A) There is a thick-walled cavity in the medial segment of the right middle lobe, with smooth edges, no lobulation or spicules, and without satellite lesions (black arrow); (B) the cavity wall shows uniform soft tissue density on plain scan (white arrow); (C) the cavity wall shows slight enhancement at arterial phase scan (white arrow); (D) the cavity wall shows moderate delayed enhancement at venous phase scan (white arrow). CT, computed tomography.

lesions (100). DR-PTB more likely involves multiple lung lobes/segments. Cavities are common and larger in size, with mostly thick-walled in DR-PTB. DR-PTB is more destructive to lung tissue and often damages the lungs (*Figure 11*).

Acknowledgments

This expert consensus is initiated by Infectious Disease Imaging Group, Infectious Disease Branch, Chinese Research Hospital Association; Infectious Diseases Group of Chinese Medical Association of Radiology; Digital Health Committee of China Association for the Promotion of Science and Technology Industrialization; Committee of AIDS Imaging of China STD and AIDS Prevention Association; Infectious Diseases Group, General Radiological Equipment Committee, China Association of Medical Equipment; and Beijing Imaging Diagnosis and Treatment Technology Innovation Alliance.

Funding: This study was supported by the National Key R&D Program of China (No. 2019YFE01214001), Shenzhen Fundamental Research Program (No. JCYJ20190813153413160), Key Research and Development Program of Guangzhou (No. 2023B03J1303), Guangzhou Science and Technology Planning Project (No. 2023A03J0994), Chongqing Medical Scientific Research Project (Joint Project of Chongqing Health Commission and Science and Technology Bureau) (No. 2023DBXM005), and Nanjing Medical Science and Technique Development Foundation (No. YKK21126).

Footnote

Conflicts of Interest: All authors have completed the ICMJE uniform disclosure form (available at https://qims.amegroups.com/article/view/10.21037/qims-23-1223/coif). The authors have no conflicts of interest to declare.

Ethical Statement: The authors are accountable for all aspects of the work in ensuring that questions related to the accuracy or integrity of any part of the work are appropriately investigated and resolved.

References

1. Global tuberculosis report 2022. Geneva: World Health Organization, 2022.
2. Wáng YXJ, Chung MJ, Skrahin A, Rosenthal A, Gabrielian A, Tartakovsky M. Radiological signs associated with pulmonary multi-drug resistant tuberculosis: an analysis of published evidences. Quant Imaging Med Surg 2018;8:161-73.
3. Li D, He W, Chen B, Lv P. Primary multidrug-resistant tuberculosis versus drug-sensitive tuberculosis in non-HIV-infected patients: Comparisons of CT findings. PLoS One 2017;12:e0176354.
4. Cheng N, Wu S, Luo X, Xu C, Lou Q, Zhu J, You L, Li B. A Comparative Study of Chest Computed Tomography Findings: 1030 Cases of Drug-Sensitive Tuberculosis versus 516 Cases of Drug-Resistant Tuberculosis. Infect Drug Resist 2021;14:1115-28.
5. LI F, Xu Z. Medical Microbiology. Beijing: People's Medical Publishing House, 2018.
6. Turner RD, Bothamley GH. Cough and the transmission of tuberculosis. J Infect Dis 2015;211:1367-72.
7. Khan MK, Islam MN, Ferdous J, Alam MM. An Overview on Epidemiology of Tuberculosis. Mymensingh Med J 2019;28:259-66.
8. Ma A, Zhao Y. The prevalence and surveillance of drug-resistant tuberculosis. Chinese Journal of Antibiotics 2018;43:502-506.
9. Miotto P, Cirillo DM, Migliori GB. Drug resistance in Mycobacterium tuberculosis: molecular mechanisms challenging fluoroquinolones and pyrazinamide effectiveness. Chest 2015;147:1135-43.
10. Chinese Society of infectious disease of Chinese Society of Radiology. Expert consensus on Imaging diagnosis of hierarchical diagnosis and treatment for tuberculosis. Electronic Journal of Emerging Infectious Diseases 2018;3:118-27.
11. World Health Organization. Meeting report of the WHO expert consultation on the definition of extensively drug-resistant tuberculosis, 27-29 October 2020. Geneva: World Health Organization, 2021.
12. Li R, Ruan Y, Li Y. Interpretation of the new definition of extensive drug-resistant tuberculosis defined by World Health Organization. Chinese Journal of Antituberculosis 2021;43:539-41.
13. The National Health and Family Planning Commission of the People's Republic of China. Criteria for the diagnosis of pulmonary tuberculosis (WS 288-2017). Electronic Journal of Emerging Infectious Diseases 2018;3:59-61.
14. Chinese Society for Tuberculosis. Interpretation of expert consensus on pathological diagnosis of tuberculosis in China. Chinese Journal of Tuberculosis and Respiratory Diseases 2017;40:419-25.
15. Feng R. Pathological diagnosis and differential diagnosis of granulomatous pulmonary disease. Chinese Journal of Tuberculosis and Respiratory Diseases 2020;43:1004-8.
16. Clinical Laboratory Committee of tuberculosis Branch of Chinese Medical Association. Expert consensus on molecular diagnosis of tuberculosis etiology. Chinese Journal of Tuberculosis and Respiratory Diseases 2018;41:688-95.
17. Professional Committee of HIV Combined with TB, Chinese Association of STD and AIDS Prevention and Control. Expert consensus on diagnosis and treatment of tuberculosis in patients with human immunodeficiency virus/acquired immunodeficiency syndrome. Electronic Journal of Emerging Infectious Diseases 2022;7:73-87.
18. Terracciano L, Brozek J, Compalati E, Schünemann H. GRADE system: new paradigm. Curr Opin Allergy Clin Immunol 2010;10:377-83.
19. Radiology Committee on Infectious and Inflammatory Disease, Chinese Research Hospital Association; Infectious Diseases Sub-branch, Radiology Branch, Chinese Medical Association; Committee on Radiology of Infection, Radiologist Branch, Chinese Medical Doctor Association; Radiology Committee on Infectious Disease, Chinese Association of STD and AIDS Prevention and Control; Radiology Subbranch on Infectious Diseases, Infectious Diseases Branch, Chinese Hospital Association; Beijing Imaging Technology Innovation Alliance; China Quality Association for Pharmaceuticals Medical Imaging Quality Research Committee. Imaging diagnostic criteria of Non-Tuberculous Mycobacterial lung disease. Journal of Chinese Research Hospitals 2021;8:1-6.
20. Pillay T, Andronikou S, Zar HJ. Chest imaging in paediatric pulmonary TB. Paediatr Respir Rev 2020;36:65-72.
21. Nel M, Franckling-Smith Z, Pillay T, Andronikou S,

Zar HJ. Chest Imaging for Pulmonary TB-An Update. Pathogens 2022;11:161.
22. Cardinale L, Parlatano D, Boccuzzi F, Onoscuri M, Volpicelli G, Veltri A. The imaging spectrum of pulmonary tuberculosis. Acta Radiol 2015;56:557-64.
23. Jeong YJ, Lee KS. Pulmonary tuberculosis: up-to-date imaging and management. AJR Am J Roentgenol 2008;191:834-44.
24. Gambhir S, Ravina M, Rangan K, Dixit M, Barai S, Bomanji J; International Atomic Energy Agency Extra-pulmonary TB Consortium. Imaging in extrapulmonary tuberculosis. Int J Infect Dis 2017;56:237-47.
25. Arora A, Bhalla AS, Jana M, Sharma R. Overview of airway involvement in tuberculosis. J Med Imaging Radiat Oncol 2013;57:576-81.
26. Skoura E, Zumla A, Bomanji J. Imaging in tuberculosis. Int J Infect Dis 2015;32:87-93.
27. Knisely BL, Broderick LS, Kuhlman JE. MR imaging of the pleura and chest wall. Magn Reson Imaging Clin N Am 2000;8:125-41.
28. Priftakis D, Riaz S, Zumla A, Bomanji J. Towards more accurate (18)F-fluorodeoxyglucose positron emission tomography ((18)F-FDG PET) imaging in active and latent tuberculosis. Int J Infect Dis 2020;92S:S85-90.
29. World Health Organization. WHO Rapid Communication WHO Rapid Communication on Systematic Screening for Tuberculosis. (2022, August 14). WHO Rapid Communication WHO Rapid Communication on Systematic Screening for Tuberculosis. 2020. Available online: https://www.who.int/publications/i/item/rapid-communication-on-the-systematic-screening-fortuberculosis
30. Deesuwan P, Autravisittikul O, Girapongsa L. Chest radiographic findings of multidrug resistant pulmonary tuberculosis in comparisons to drug-sensitive pulmonary tuberculosis in non-HIV patient. Region 4-5 Med J 2015;34:66-78.
31. Zahirifard S, Amiri MV, Karam MB, Mirsaeidi SM, Ehsanpour A, Masjedi MR. The radiological spectrum of pulmonary multidrug-resistant tuberculosis in HIV-negative patients. Iran J Radiol 2013;1:161-7.
32. Dholakia YN, D'souza DT, Tolani MP, Chatterjee A, Mistry NF. Chest X-rays and associated clinical parameters in pulmonary tuberculosis cases from the National Tuberculosis Programme, Mumbai. Infect Dis Rep 2012;4:e10.
33. Majdawati A, Icksan AG, Lolong D. Comparison of chest X-ray lesion characteristics of multidrug-resistant tuberculosis and non-tuberculous mycobacterial infection. Pol J Radiol 2019;84:e162-70.
34. Icksan AG, Napitupulu MRS, Nawas MA, Nurwidya F. Chest X-Ray Findings Comparison between Multi-drug-resistant Tuberculosis and Drug-sensitive Tuberculosis. J Nat Sci Biol Med 2018;9:42-6.
35. Yang F, Yu H, Kantipudi K, Karki M, Kassim YM, Rosenthal A, Hurt DE, Yaniv Z, Jaeger S. Differentiating between drug-sensitive and drug-resistant tuberculosis with machine learning for clinical and radiological features. Quant Imaging Med Surg 2022;12:675-87.
36. Flores-Treviño S, Rodríguez-Noriega E, Garza-González E, González-Díaz E, Esparza-Ahumada S, Escobedo-Sánchez R, Pérez-Gómez HR, León-Garnica G, Morfín-Otero R. Clinical predictors of drug-resistant tuberculosis in Mexico. PLoS One 2019;14:e0220946.
37. Sulistijawati RS, Icksan AG, Lolong DB, Nurwidya F. Thoracic Radiography Characteristics of Drug Sensitive Tuberculosis and Multi Drug Resistant Tuberculosis: A Study of Indonesian National Tuberculosis Prevalence Survey. Acta Medica (Hradec Kralove) 2019;62:24-9.
38. Chuchottaworn C, Thanachartwet V, Sangsayunh P, Than TZ, Sahassananda D, Surabotsophon M, Desakorn V. Risk Factors for Multidrug-Resistant Tuberculosis among Patients with Pulmonary Tuberculosis at the Central Chest Institute of Thailand. PLoS One 2015;10:e0139986.
39. Mehrian P, Farnia P, Jalalvand D, Chamani MR, Bakhtiyari M. Computerised tomography scan in multi-drug-resistant versus extensively drug-resistant tuberculosis. Pol J Radiol 2020;85:e39-44.
40. Liang R, Fang W, Ren H, Li H, Zhang H, Li C. Analysis of CT features of drug-resistant tuberculosis pulmonary tuberculosis with cavity. Chinese Journal of Antituberculosis 2021;43:341-5.
41. Cheon H. Comparison of CT findings of between MDR-TB and XDR-TB: A propensity score matching study. Imaging in Medicine 2017;9:125-9.
42. Chen G, Cheng G, Zhu S, Zeng L, Wen Z, Zhuang Y.CT scanning of mono-resistant pulmonary tuberculosis during initial treatment. Electronic Journal of Emerging Infectious Diseases 2018;3:111-4.
43. Zhang Z, Ren G, Tan J, Li Y, Xu L. CT features of drug rifampicin resistant tuberculosis. Guide of China Medicine 2015;13:64-5.
44. Li H, Zhou X, Lv Y, Yu X, Li F, He W, Chen B, Wang D, Zhou Z, Ning F. Prediction of multiple drug resistant pulmonary tuberculosis against drug sensitive pulmonary tuberculosis by CT nodular consolidation sign. bioRxiv

2019. doi: 10.1101/833954
45. Shi W, Wu J, Tan Q, Hu CM, Zhang X, Pan HQ, Yang Z, He MY, Yu M, Zhang B, Xie WP, Wang H. Plasma indoleamine 2,3-dioxygenase activity as a potential biomarker for early diagnosis of multidrug-resistant tuberculosis in tuberculosis patients. Infect Drug Resist 2019;12:1265-76.
46. Li C, Lv S, Wang H, Shu W, Yang C, Li T, Yang K, Yan X. CT manifestations of multidrug-resistant pulmonary tuberculosis patients and their relationship with CD4 cells. Chinese Journal of Antituberculosis 2017;39:597-603.
47. Luo L, Li B, Chu H, Huang D, Zhang Z, Zhang J, Gui T, Xu L, Zhao L, Sun X, Xiao H. Classification and imaging manifestations of drug-resistant pulmonary tuberculosis. Electronic Journal of Emerging Infectious Diseases 2019;4:42-7.
48. Dong Z, Chen H, Hong J, Ao G. Pulmonary multidrug resistant tuberculosis as demonstrated on thin-slice computed tomography. Chinese Journal of Clinicians (Electronic Edition) 2013;7:9494-7.
49. Joshi AR, Mishra S, Sankhe AP, Bajpai AR, Firke V. HRCT Spectrum of Pulmonary Multidrug-Resistant Tuberculosis in HIV Negative Patients: A Study in Indian Population. International Journal of Science and Research 2017;6:596-600.
50. Yang J, Lv S, Tang G, Shu W, Wang H, Yang C, Liu X, Li C. Analysis of CT findings in patients with initial and retreated multidrug-resistant tuberculosis. Chinese Journal of Antituberculosis 2020;42:38-43.
51. Ma L, Zheng Q, Lv P, Li H, Liu Y, Yin X, Huo L. Pulmonary multi-drug resistant tuberculosis: a radiological review. Electronic Journal of Emerging Infectious Diseases 2021;6:58-65.
52. Song QS, Zheng CJ, Wang KP, Huang XL, Tartakovsky M, Wáng YXJ. Differences in pulmonary nodular consolidation and pulmonary cavity among drug-sensitive, rifampicin-resistant and multi-drug resistant tuberculosis patients: a computerized tomography study with history length matched cases. J Thorac Dis 2022;14:2522-31.
53. Li CH, Fan X, Lv SX, Liu XY, Wang JN, Li YM, Li Q. Clinical and Computed Tomography Features Associated with Multidrug-Resistant Pulmonary Tuberculosis: A Retrospective Study in China. Infect Drug Resist 2023;16:651-9.
54. Yeom JA, Jeong YJ, Jeon D, Kim KI, Kim CW, Park HK, Kim YD. Imaging findings of primary multidrug-resistant tuberculosis: a comparison with findings of drug-sensitive tuberculosis. J Comput Assist Tomogr 2009;33:956-60.
55. Cao P, Liang K, Yuan J, Li Y, Chen R, Zheng Z, Wu Q. Analysis of CT findings in patients with initial and retreated cavernous rifampicin-resistant tuberculosis. Chinese Journal of Antituberculosis 2021;43:694-701.
56. Cha J, Lee HY, Lee KS, Koh WJ, Kwon OJ, Yi CA, Kim TS, Chung MJ. Radiological findings of extensively drug-resistant pulmonary tuberculosis in non-AIDS adults: comparisons with findings of multidrug-resistant and drug-sensitive tuberculosis. Korean J Radiol 2009;10:207-16.
57. Lee ES, Park CM, Goo JM, Yim JJ, Kim HR, Lee HJ, Lee IS, Im JG. Computed tomography features of extensively drug-resistant pulmonary tuberculosis in non-HIV-infected patients. J Comput Assist Tomogr 2010;34:559-63.
58. David HL. Probability distribution of drug-resistant mutants in unselected populations of Mycobacterium tuberculosis. Appl Microbiol 1970;20:810-4.
59. Qi LP, Chen KN, Zhou XJ, Tang L, Liu YL, Li XT, Wang J, Sun YS. Conventional MRI to detect the differences between mass-like tuberculosis and lung cancer. J Thorac Dis 2018;10:5673-84.
60. De Backer AI, Mortelé KJ, Van Den Heuvel E, Vanschoubroeck IJ, Kockx MM, Van de Vyvere M. Tuberculous adenitis: comparison of CT and MRI findings with histopathological features. Eur Radiol 2007;17:1111-7.
61. Moon WK, Im JG, Yu IK, Lee SK, Yeon KM, Han MC. Mediastinal tuberculous lymphadenitis: MR imaging appearance with clinicopathologic correlation. AJR Am J Roentgenol 1996;166:21-5.
62. Qi W, Wu Y, Zhu X, Wan T, Tang X, He Y. The clinical application value of high filed MRI in the examination and diagnosis of pulmonary tuberculosis. Electronic Journal of Emerging Infectious Diseases 2020;5:212-4.
63. Rizzi EB, Schinina' V, Cristofaro M, Goletti D, Palmieri F, Bevilacqua N, Lauria FN, Girardi E, Bibbolino C. Detection of Pulmonary tuberculosis: comparing MR imaging with HRCT. BMC Infect Dis 2011;11:243.
64. Yu WY, Zhang QQ, Xiao Y, Tan WG, Li XD, Lu PX. Correlation between 18F-FDG PET CT SUV and symptomatic or asymptomatic pulmonary tuberculosis. J Xray Sci Technol 2019;27:899-906.
65. Yu WY, Lu PX, Assadi M, Huang XL, Skrahin A, Rosenthal A, Gabrielian A, Tartakovsky M, Wáng YXJ. Updates on (18)F-FDG-PET/CT as a clinical tool for tuberculosis evaluation and therapeutic monitoring. Quant

Imaging Med Surg 2019;9:1132-46.
66. Verkuijl S, Sekadde MP, Dodd PJ, Arinaitwe M, Chiang SS, Brands A, Viney K, Sismanidis C, Jenkins HE. Addressing the Data Gaps on Child and Adolescent Tuberculosis. Pathogens 2022;11:352.
67. Shen A, Jiao W. Prevalence and drug resistance of tuberculosis in children. Chinese Journal of Applied Clinical Pediatrics 2016;31:269-71.
68. Song M, Fang W, Han Y, Feng H. Analysis of CT features of drug-resistant tuberculosis in children. Journal of Tuberculosis and Lung Disease 2020;9:58-63.
69. Manikkam S, Archary N, Bobat R. Chest X-ray patterns of pulmonary multidrug-resistant tuberculosis in children in a high HIV-prevalence setting. South African Journal of Radiology 2016;20:a829.
70. Liu F, Shen C, Sun L, Rao X, Ma Y, Meng C, Pan Y, Li G, Jiao A. Clinical and bronchoscopic manifestations of tracheobronchial tuberculosis in children. Chinese Journal of Antituberculosis 2018;40:917-23.
71. Li H, Zhao S. Diagnosis progress of pulmonary tuberculosis in children. Chinese Journal of Antituberculosis 2018;40:259-62.
72. Santiago-García B, Blázquez-Gamero D, Baquero-Artigao F, Ruíz-Contreras J, Bellón JM, Muñoz-Fernández MA, Mellado-Peña MJ; EREMITA Study Group. Pediatric Extrapulmonary Tuberculosis: Clinical Spectrum, Risk Factors and Diagnostic Challenges in a Low Prevalence Region. Pediatr Infect Dis J 2016;35:1175-81.
73. Wang Y, Zhao S, Yu T, Zhang H, Liu Z, Sun J, Zeng J, Peng Y. Analysis of clinical characteristics of pulmonary tuberculosis in children based on CT typing method. Chinese Journal of Antituberculosis 2018;40:940-3.
74. Yang LY, Huang YF, Yu Y, Liu F. Clinical epidemiological characteristics of 920 children with pulmonary tuberculosis. Journal of Clinical Pediatrics 2019;37:413-7.
75. Xi Y, Tang J, Qiao R, Sun F, Yu Y. Investigation of drug resistance status and risk factors of multi-drug resistance in 249 aged pulmonary tuberculosis patients. Chinese Journal of Antituberculosis 2021;43:636-41.
76. Ye M. Clinical analysis of 90 aged drug-resistant pulmonary tuberculosis. Journal of Clinical Pulmonary Medicine 2010;15:1801-2.
77. Tao M, Yang Q, Zhang L, Li Y. Clinical curative effect and outcomes of multidrug-resistant tuberculosis in elderly patient. Anhui Medical and Pharmaceutical Journal 2017;21:2185-8.
78. Li Y. Clinical efficacy of moxifloxacin in the treatment of elderly multidrug-resistant pulmonary tuberculosis patients. China Practical Medical 2016;11:203-4.
79. Lan Y, Liu M, Zhang J, Li N, Chen L. Analysis of clinical and drug resistance characteristics in elderly pulmonary tuberculosis patients. Chinese Journal of Gerontology 2015;35:5203-4.
80. Luo X, Yang C, Cui H. Comparative analysis of clinical characteristics and drug resistance in elderly versus non-elderly patients with recurrent smear positive pulmonary tuberculosis. Chinese Journal of Geriatrics 2020;39:1419-23.
81. Rumende CM, Mahdi D. Role of combined procalcitonin and lipopolysaccharide-binding protein as prognostic markers of mortality in patients with ventilator-associated pneumonia. Acta Med Indones 2013;45:89-93.
82. Ben-Abraham R, Weinbroum AA, Roizin H, Efrati O, Augarten A, Harel R, Moreh O, Barzilay Z, Paret G. Long-term assessment of pulmonary function tests in pediatric survivors of acute respiratory distress syndrome. Med Sci Monit 2002;8:CR153-7.
83. Li H, Zhang Y, Cheng J. Varieties of CT Manifestations of Pulmonary Tuberculosis in AIDS Patients and Correlation with CD4~+T Lymphocyte Count. Radiologic Practice 2009;24:959-63.
84. Xiao G, Xiao Y, Chen X, Li B, Su H. Clinicopathological features of AIDS-related opportunistic infectious diseases. Academic Journal of Guangzhou Medical College 2019;47:22-8.
85. Xie Z, Li H, Song M, Fang W, Liu Z. Comparative analysis of CT images of non-tuberculosis pulmonary disease, active pulmonary tuberculosis and multi-drug resistant pulmonary tuberculosis. Journal of Medical Imaging 2020;30:2224-7.
86. Wang D, Li Y, Wei Y, Ma J, Gao Y, Liu M, Zhang H, Li J. Meta-analysis of Clinical and Imaging Features of Nontuberculous Mycobacterial Lung Disease and Tuberculosis. Practical Clinical Journal of Integrated Traditional Chinese and Western Medicine 2021;21:1-4, 71.
87. Yu T, Shen X, Long X, Meng J, Chen X. Comparative analysis of CT images of non-tuberculous mycobacterium and multidrug-resistant pulmonary tuberculosis. Tianjin Medical Journal 2017;45:628-31.
88. Li C, Sun C, Jin W. Comparation of CT imaging features between non-tuberculous mycobacterium tuberculosis and multi-drug resistant tuberculosis. Clinical Focus 2021;36:530-4.
89. Qin Z, Ma G. Non-tuberculous mycobacterial pulmonary disease requires more attention. Chinese Journal of New Clinical Medicine 2021;14:13-8.

90. Zeng Y, Zhai XL, Wáng YXJ, Gao WW, Hu CM, Lin FS, Chai WS, Wang JY, Shi YL, Zhou XH, Yu HS, Lu XW. Illustration of a number of atypical computed tomography manifestations of active pulmonary tuberculosis. Quant Imaging Med Surg 2021;11:1651-67.
91. Ellis SM, Hansell DM. Imaging of Non-tuberculous (Atypical) Mycobacterial Pulmonary Infection. Clin Radiol 2002;57:661-9.
92. Kahkouee S, Esmi E, Moghadam A, Karam MB, Mosadegh L, Salek S, Tabarsi P. Multidrug resistant tuberculosis versus non-tuberculous mycobacterial infections: a CT-scan challenge. Braz J Infect Dis 2013;17:137-42.
93. Anjos LRBD, Parreira PL, Torres PPTS, Kipnis A, Junqueira-Kipnis AP, Rabahi MF. Non-tuberculous mycobacterial lung disease: a brief review focusing on radiological findings. Rev Soc Bras Med Trop 2020;53:e20200241.
94. Xu J, Zhang X, Chen Z. Comparative analysis of CT findings between non-tuberculous mycobacterial pulmonary disease and secondary pulmonary tuberculosis. Electronic Journal of Emerging Infectious Diseases 2020;5:113-7.
95. Luo W, Zhong C, Wang J. Analysis of imaging characteristics and changes in drug-resistant pulmonary tuberculosis patients. Journal of Imaging Research and Medical Applications 2021;5:219-20, 222.
96. Xu Y, Liu H. Image identification of invasive pulmonary aspergillosis and invasive pulmonary tuberculosis. Journal of Imaging Research and Medical Applications 2021;5:39-41.
97. Zhong Z. Clinical manifestations and CT imaging diagnosis analysis of pulmonary aspergillosis. World Latest Medicine Information 2016;16:127, 130.
98. Ohba H, Miwa S, Shirai M, Kanai M, Eifuku T, Suda T, Hayakawa H, Chida K. Clinical characteristics and prognosis of chronic pulmonary aspergillosis. Respir Med 2012;106:724-9.
99. Zheng G, Zhang Q, Tan W, Deng Q, Chen P, Su D, Yu W, Wu S, Lu P. Clinical imaging analysis of inactive tuberculosis combined with aspergillosis of the lung. Electronic Journal of Emerging Infectious Diseases 2018;3:34-36, 40.
100. Qu Y, Liu G, Ghimire P, Liao M, Shi H, Yang G, Xu L, Wang G. Primary pulmonary cryptococcosis: evaluation of CT characteristics in 26 immunocompetent Chinese patients. Acta Radiol 2012;53:668-74.

Cite this article as: Xu CJ, Lu PX, Li CH, He YL, Fang WJ, Xie RM, Jin GQ, Lu YB, Zheng QT, Zheng GP, Lv SX, Huang H, Li L, Ren M, Shi YX, Wen XN, Li L, Wei FJ, Hou DL, Lv Y, Shan F, Wu ZC, Hu ZL, Zhang XR, Liu DX, Shi WY, Li HR, Zhang N, Song M, Zhang X, Deng YY, Li J, Liu Q, Li D, Zhao L, Chen BD, Shi YB, Jiang FL, Tang X, Wu LJ, Ma W, Xu XY, Li HJ. Chinese expert consensus on imaging diagnosis of drug-resistant pulmonary tuberculosis. Quant Imaging Med Surg 2024;14(1):1039-1060. doi: 10.21037/qims-23-1223

